Measuring Boltzmann's constant using video microscopy of Brownian motion

Paul Nakroshis,[a] Matthew Amoroso, Jason Legere, and Christian Smith
Department of Physics, University of Southern Maine, Portland, Maine 04104-9300

(Received 29 July 2002; accepted 6 December 2002)

Boltzmann's constant k was measured by observing the Brownian motion of polystyrene spheres in water. An inexpensive monochrome CCD camera and video card were used to create a video of the spheres' motion. After preprocessing the images, custom routines were used to examine the video and to identify and track the particles from one frame to the next. From the mean squared displacement of the particles versus time, we extracted the value of k from the slope, assuming that the drag force on an individual sphere is well modeled by Stokes' law. By averaging over 107 particles, we obtained $k=(1.415\pm0.04)\times10^{-23}$ J/K. © *2003 American Association of Physics Teachers.*
[DOI: 10.1119/1.1542619]

I. INTRODUCTION

Brownian motion was first systematically observed by the botanist Robert Brown in 1827 and refers to the random motion of colloidal particles suspended in water.[1] In 1905, Einstein argued that this motion is direct evidence for the atomic nature of matter and that the mean square displacement of colloidal particles is the primary observable quantity.[2–4] Because of the then recent invention of the ultramicroscope, Perrin was able to make precise measurements of submicron particles and confirm almost all of Einstein's predictions for which Perrin was awarded the Nobel Prize in physics in 1926.[5,6] Einstein's and Perrin's efforts helped raise the status of atoms from useful hypothetical objects to objects whose existence could no longer be denied.

Brownian motion is relatively easy to observe with a light microscope, but until the advent of video and computer technology,[7] it has been difficult to make quantitative measurements of the motion of colloidal particles. Because of these recent technological advances, research into the dynamics of colloidal particles is now common. Typically, such work entails the use of expensive ($>$\$10 000) microscopes and video systems,[8] as well as extensive processing of thousands of images to obtain a sufficient statistical sample size for research quality results. These factors have made undergraduate laboratory experiments on Brownian motion rare. Aside from Refs. 9 and 10, which discuss a demonstration of Brownian motion and the manual tracking of the particles on a video monitor, we found only one other published undergraduate experiment on Brownian motion.[11] The latter paper incorporates video capture technology, but both Refs. 9 and 11 track only 20 particles (due to the tedium of the manual tracking of particles via acetate overlays or mouse clicks), resulting in relatively large uncertainties in the mean square displacement of the suspended particles. Reference 10 uses hundreds of individual displacements and their distribution, but does not keep track of the cumulative mean squared displacement as we do.

In this paper, we describe an upper level undergraduate laboratory experiment in which automated computer based video microscopy of 1.02 μm polystyrene spheres is used to obtain an estimate of Boltzmann's constant k which is good to within 5%. Our results are based on tracking 107 spheres at 5 Hz for a total of 12.8 s—significantly more data than the work of Refs. 9 and 11. Our setup is relatively inexpensive, the most expensive item being the Labview[12] software used to track the particles.

We will provide sufficient information about the experimental setup to allow the reader to incorporate it into an upper level undergraduate laboratory course. We also discuss features of the experimental design that are necessary to consider in order to avoid hydrodynamic sphere–wall couplings and sphere–sphere couplings that could significantly alter the experimentally determined value for k if not taken into account.

II. THEORETICAL PICTURE

To understand the motion of a colloidal particle, we note that each water molecule experiences about 10^{11} collisions per second. Hence, when we image the particle positions with even the fastest video cameras, each particle will have undergone millions of collisions between images, and we can effectively treat the particle motion from one frame to the next as a sequence of independent events.

We first derive the ensemble average square displacement for particles subject to random impulses and a dissipative drag force $-\mu\dot{x}$.[13,14] In one dimension, the mean squared displacement is given by

$$\frac{d\langle x^2\rangle}{dt}=\frac{2kT}{\mu}, \tag{1}$$

where μ is the linear drag coefficient. Because we are using spherical particles of radius a, we use Stoke's law to write μ as

$$\mu=6\pi\eta a, \tag{2}$$

where η is the viscosity of the fluid, and a is the particle's radius.

Because there is nothing special about the motion in the x direction, we expect the mean squared displacement in two dimensions to have a similar form

$$\langle R^2\rangle=\frac{4kT}{6\pi\eta a}t. \tag{3}$$

Hence, by plotting $\langle R^2\rangle$ as a function of time, we expect a straight line through the origin whose slope can be used to

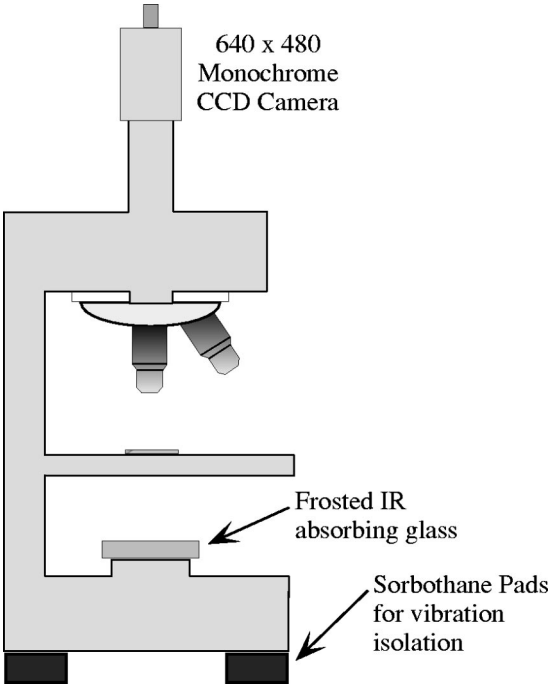

Fig. 1. Schematic of microscope setup. The output of the CCD camera goes to the XClaimVR capture card.

obtain Boltzmann's constant k. Equation (3) also is commonly written as

$$\langle R^2 \rangle = 4Dt, \tag{4}$$

where $D = kT/6\pi\eta a$ is the self-diffusion constant.

Another method of determining k relies on examining the distribution of step lengths for many particles in the x or y directions (Ref. 18). The probability density for finding a one-dimensional displacement Δ is

$$P(\Delta) = \sqrt{\frac{1}{2\pi\sigma^2}}\, e^{-\Delta^2/2\sigma^2}, \tag{5}$$

where $\sigma = \sqrt{2D\tau}$ and τ is the time interval between position measurements. Therefore, we can obtain D (and hence k) by fitting Eq. (5) to a normalized histogram of the step lengths of the spheres.

III. EXPERIMENTAL METHOD

We used an inexpensive American Optical Spencer Microscope, which comes with a binocular head which we removed and used the included video head to mount a 640 $\times$480 pixel monochrome CCD (Watec-502A). A c-mount extension tube (available from Edmund Scientific) is needed to adapt the camera to the video head. The image from the 45$\times$ objective lens is directly imaged onto the CCD. We calibrated the image using a 15 000 lines/in diffraction grating and obtained values of 5.024 μm/pixel (horizontal) and 5.031 μm/pixel (vertical). To minimize the thermal heating of our samples, we used a piece of infrared absorbing glass (from Edmund Scientific) and placed it below the condensing lens of the microscope. To improve the uniformity of the illumination, we first frosted the infrared glass by grinding it with 220 grit silicon carbide abrasive. Figure 1 shows the microscope setup, which includes sorbothane pads to help reduce the effects of vibration. We connected the output of the CCD camera to a XClaimVR video capture card,[15] which included software to allow us to observe images in real time and make QuickTime videos.

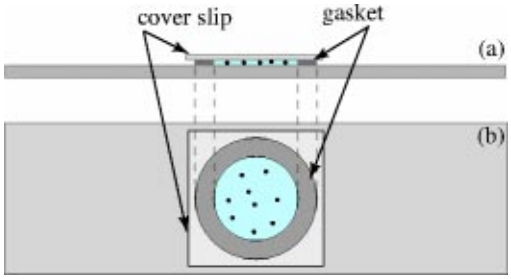

Fig. 2. Illustration of slide mounting system. The gasket was a self-stick hole reinforcement with thickness 80 μm.

To observe Brownian motion, we used 1.02 μm diameter polystyrene microspheres from Bangs Laboratories.[16] The spheres come suspended in water and a 5 ml volume (the smallest quantity available) provides an ample number of spheres to prepare thousands of samples for viewing. In fact, the sphere density was so high that we had to dilute a small quantity by a factor of 200 so that the spheres did not collide too frequently with each other. We found that after sitting overnight, the spheres tended to settle out of suspension and aggregate; by inserting an ultrasonic probe into the sample, we were able to successfully disperse the solution. The spheres appear to be unharmed by this procedure.

We created a custom observation cell by placing a self-sticking plastic hole reinforcement (normally used to reinforce 3-hole punched paper) onto a 1″$\times$3″ microscope slide (Fig. 2). One drop of the microsphere solution (from the needle of a 3 cc syringe) was placed on a cover slip and the cover slip was inverted (the drop adheres via cohesive forces to the glass) and placed on the glass slide in the center of the plastic reinforcement. The cover slip was gently pressed and a seal was formed between the gasket, the slide, and the cover slip. We observed the slide on the computer using the software that came with the video capture card. If the sample exhibited any evidence of a coherent macroscopic oscillation or flow, we discarded the slide and make a new one. Our experience is that if an air bubble is visible in the central circular area, there will be visible flow which will make the data from such a slide unusable. Although we have not quantitatively studied the motion in such a slide, our qualitative observation is that the fluid appears to oscillate, and we speculate that the trapped air bubble acts like a spring and induces macroscopic oscillations in the fluid that are observable by watching the spheres.

Once we have an acceptable sample, we make several QuickTime videos of the motion. To insure the best image quality, we do not use any compression and save the videos in tiff format. Some amount of experimentation with the microscope illumination level is needed to get the best image contrast; we found that the QuickTime videos end up darker than the real time display on the monitor would suggest. The data in this paper was sampled at 5 frames/s for a total of 12.8 s. We made four slides and made three videos of each slide for a total of 12 videos. However, we found that the videos based from slides one and four had an excessive drift,

and we discarded these six data runs. The remaining two slides left us with six videos constituting a total of 142 Mb of video data.

A. Hydrodynamic effects

We use the gasket method outlined in Sec. III so that we can minimize the hydrodynamic coupling of the spheres to the slide and to the cover slip.[17,18] For a single sphere of radius a far from two parallel walls, the modified self-diffusion constant is given by

$$D' = D\left[1 - \frac{9a}{16}\left(\frac{1}{x_1} - \frac{1}{x_2}\right)\right], \tag{6}$$

where x_1 and x_2 are the distances from the sphere to the two walls. We used the micrometer adjustment on the microscope to insure that the focal plane is in the middle of the observing cell. Hence, the 0.5 μm radius spheres we observe nominally sit at $x_1 \approx x_2 \approx 40$ μm from the cell walls, and from Eq. (6) we find that the self-diffusion constant is systematically reduced by $\approx 1.4\%$. We will therefore need to *increase* our measured value of k by this amount to compensate for this effect.

We used a dilute suspension of spheres so that we can minimize the effects of sphere–sphere interactions. This effect is quantified by the parameter ρ, which is the ratio of the center to center separation distance, r, to the sphere radius, a. As discussed in Ref. 18, the dominant effect on the self-diffusion constant is along the line connecting the centers of two spheres, and is given by

$$D'_{\|} = D\left[1 - \frac{15}{4\rho^4} + O(\rho^{-6})\right]. \tag{7}$$

The average sphere separation in our slides was greater than 3 diameters and hence this sphere–sphere coupling results in a 0.02 percent correction to the diffusivity, which we ignored. The correction to the diffusion perpendicular to this center–center line is order ρ^{-6} and is negligible for the purposes of this experiment.

B. Data extraction

There are two general methods for extracting the data from the Quicktime videos. The first involves a manual method such as the program VideoGraph,[19] and we used it for the initial development of our experiment. With VideoGraph, one opens a QuickTime video, calibrates the image, and then specifies how many objects to track. Then, on the first frame of the video, one manually centers the cursor over each particle and clicks, repeating for as many particles as are being tracked. When finished, the program advances to the next frame, and the process is repeated through the last frame of the video. When done, VideoGraph displays a table of x and y positions which can then be analyzed.

The VideoGraph analysis is useful primarily because it is easy to implement. We can obtain a small data set to analyze relatively easily. However, there are serious disadvantages. First, we need to remember the positions and the order in which the particles were clicked. Each particle must be chosen in the same sequence from one frame to the next if the data for each particle is to be meaningful. Practically speaking, this requirement limits the number of particles that one can track to about 5 or so. Any more than this, and we found that it was difficult to remember which particles were tracked and the order in which they were chosen. The second disadvantage to this method is the shear tedium of tracking the particles by hand. For instance, if the data in this paper was obtained by VideoGraph, we would have had to execute 6848 mouse clicks.

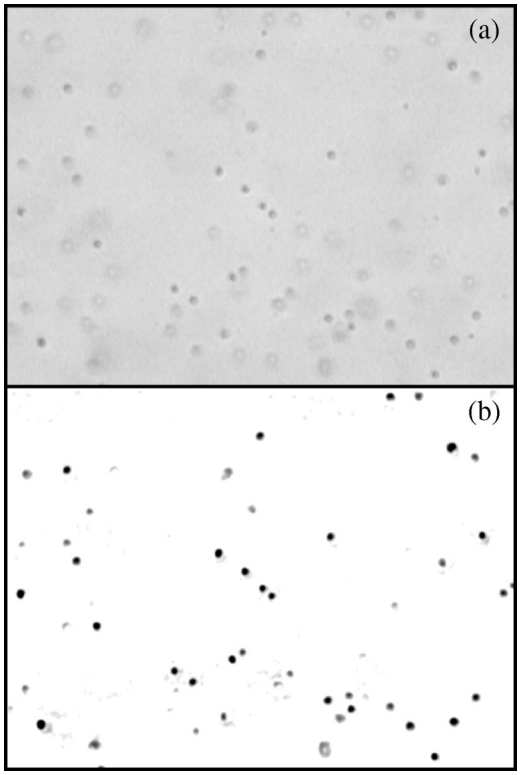

Fig. 3. Raw image (a) of 1 μm spheres and the processed image (b) resulting from subtracting the background, smoothing, and adjusting the contrast.

Because of the limitations of VideoGraph, we automated the extraction of data from the QuickTime videos. Our method involves (a) preparing the videos for processing by subtracting the background, improving the image contrast, and saving each video as a sequence of images, and (b) finding the positions of all particles that can be tracked from the beginning of the video to the end.

We prepared each video for processing by eliminating the effects of nonuniform illumination and other fixed image deformations (such as nonuniform CCD pixel sensitivity or dust specks on the CCD window). To accomplish this, we made a short video of a blank slide under the same illumination conditions as the real samples. We used the freeware program ImageJ[20] to open this short video and averaged the frames together to create a background image that we then subtracted from each frame of every video. We then autocontrasted the video, applied a mean filter (3 pixel radius, which is about the size of a sphere in our image), made a manual adjustment to the contrast and brightness in the video, and then saved each video as a set of sequentially numbered images. The mean filter serves to blur details smaller than the size of one sphere, as well as further blur the images of out of focus spheres. Figure 3 shows an image before and after this processing.

Our custom LabView routines[21] operated on sequentially numbered images (for instance frame001, frame002, etc.). Because each particle's image is circular, our routine simply

searches for all circles in the image and defines the particle position as the coordinate of the center of the circle. The difficult part of this process lies in tracking particles from one frame to the next. We use very conservative constraints to link particles into trajectories; we eliminate any particles that come within seven pixels (1.4 μm) of each other, and we eliminate any particles that travel more than seven pixels between frames. These numbers are based on theoretical expectations for the Brownian motion of 1 μm spheres and would have to be adjusted for different diameter spheres.

Because some of the spheres collide with or are stuck to other spheres, the first constraint has the effect of limiting our data to isolated particles. Because particles occasionally move far enough out of focus to disappear (or spontaneously appear when previously absent), the second constraint prevents us from identifying a particle that disappears with one that simultaneously reappears close to, but unphysically far from, the disappearing particle.

After processing a video, our LabView routines produce a text file for each frame of the video. The columns are: horizontal position, vertical position, and radius (all in pixels), and particle area (in square pixels). Each time a new particle is detected, a new row is added. If a particle disappears, the x and y positions, the radius, and the area are set to zero. Hence, the number of rows in each text file must either stay the same or increase as successive frames are analyzed. The last remaining piece is to sort through these files and extract the desired particle trajectories. To simplify this analysis, we select only those particles that are present in every frame of the video.

IV. ANALYSIS

A. Determination of k from the root-mean-square displacement

We read, analyze, and plot the data from LabView (or VideoGraph) with the scientific graphics package IgorPro.[22] We subtract off the initial x and y positions for each particle, so that for the ith particle at time t, we have $\Delta x_i(t)=x_i(t)-x_i(0)$ and $\Delta y_i(t)=y_i(t)-y_i(0)$. The square displacement of the ith particle at time t is therefore

$$[\Delta R_i(t)]^2=[\Delta x_i(t)]^2+[\Delta y_i(t)]^2. \tag{8}$$

To obtain Boltzmann's constant, we need to plot the mean squared displacement versus time, so we calculate the time-dependent quantity

$$\langle R^2\rangle \equiv \frac{1}{N}\sum_{i=1}^{N}[\Delta R_i(t)]^2, \tag{9}$$

where N is the number of particles tracked (107 in our case). Figure 4 shows our data.

From the slope s shown in Fig. 4, we use Eq. (3) to obtain Boltzmann's constant, k,

$$k=\frac{6\pi\eta a s}{4T}. \tag{10}$$

The coefficient of viscosity is a nonlinear function of temperature, so we used data from the CRC Handbook[23] to approximate the viscosity at the temperature of our sample ($22.86\pm0.03\,^\circ$C). We fit the data shown in Table I to an exponential between 10 °C and 40 °C and interpolated it to obtain the value shown in Eq. (11),

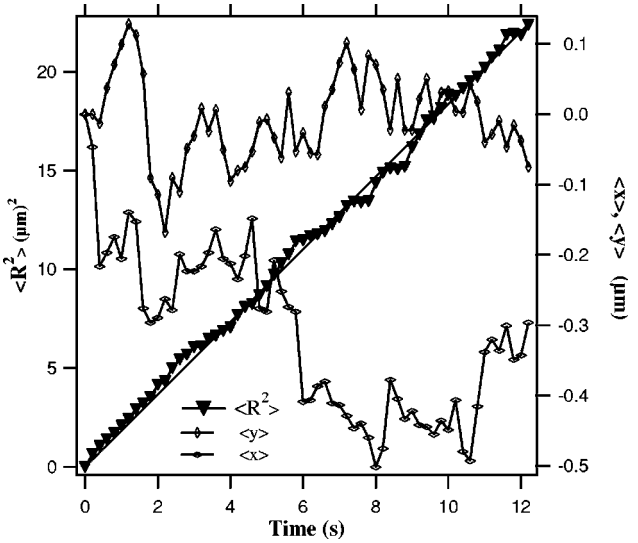

Fig. 4. Mean square displacement for 107 polystyrene spheres of diameter 1.02 μm. Also shown are the average horizontal and vertical displacements, as well as a linear fit to the average R^2 data. This fit is constrained to go through zero. The slope of this fit is $s=1.836\pm0.02\ \mu\text{m}^2/\text{s}$.

$$\eta=936\pm15\ \mu\text{Pa s}. \tag{11}$$

We also have that

$$a=0.51\pm0.01\ \mu\text{m}, \tag{12}$$

$$T=296.01\pm0.3\ \text{K}, \tag{13}$$

$$s=1.836\pm0.02\ \mu\text{m}^2/\text{s}. \tag{14}$$

We convert the above values to SI units and substitute them into Eq. (10) to obtain

$$k=(1.395\pm0.04)\times10^{-23}\ \text{J/K}\quad(\text{uncorrected}), \tag{15}$$

where the uncertainty in k was obtained by adding the fractional uncertainties in quadrature:

$$\left(\frac{\Delta k}{k}\right)^2=\left(\frac{\Delta\eta}{\eta}\right)^2+\left(\frac{\Delta a}{a}\right)^2+\left(\frac{\Delta s}{s}\right)^2+\left(\frac{\Delta T}{T}\right)^2. \tag{16}$$

However, because of the hydrodynamic effects of the parallel walls on the spheres, we have to increase this estimate by 1.4%, which yields a final value for k:

$$k=(1.415\pm0.04)\times10^{-23}\ \text{J/K}\quad(\text{corrected}). \tag{17}$$

As a quantitative check of the data, we also calculated the mean horizontal and vertical displacements of the particles as functions of time, that is,

Table I. Viscosity of water as a function of temperature as taken from the 1991–1992 CRC Handbook of Chemistry and Physics (Ref. 23). We fit this data to an exponential to obtain a value for the viscosity at 22.86 °C.

Temperature (°C)	Viscosity (μPa s)
0	1793.0
10	1307.0
20	1002.0
30	797.7
40	653.2

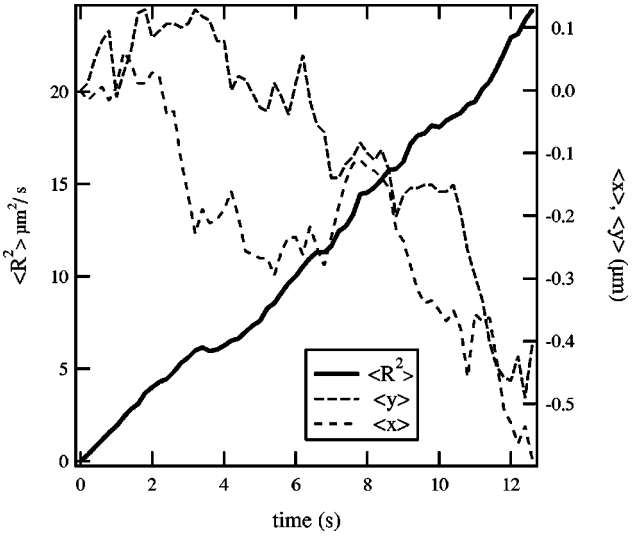

Fig. 5. Simulated data based on a mean step length of 0.61 μm every 0.2 s. This step length is based on the slope obtained in Fig. 4.

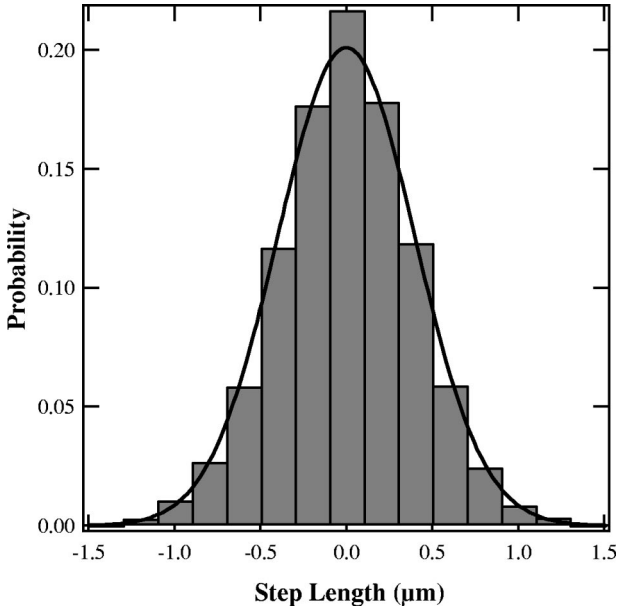

Fig. 6. The distribution of step lengths for all 107 particles. The time interval between measurements is 0.2 s. The bin width is 0.2 μm. A Gaussian fit of the form listed in Eq. (5) yields a diffusion constant of 0.396 $\pm$0.06 μm^2/s.

$$\langle \Delta x \rangle \equiv \frac{1}{N} \sum_{i=1}^{N} \Delta x_i(t)$$

and

$$\langle \Delta y \rangle \equiv \frac{1}{N} \sum_{i=1}^{N} \Delta y_i(t). \tag{18}$$

As N approaches infinity, we expect these averages to approach zero for all times. Figure 4 shows that the average horizontal and vertical displacements are not identically zero, so we need some method of deciding if these displacements are consistent with zero drift.

To do so, we wrote a program (in Igor Pro) to simulate a zero drift random walk with the same number of random walkers and steps present in each slide. We used the slope from Fig. 4 to calculate the diffusion constant and hence an average step length in 0.2 s (our sampling interval) as 0.61 μm. The simulated data in Fig. 5 is quantitatively similar to the actual data, leading us to assume that there are no obvious drifts in our data. This method also was used to eliminate particles from slides 1 and 4 that had maximum average displacements well beyond what the simulation suggests would be reasonable for these slides.

B. Alternate determination of k via probability distribution

We also used our data to plot a distribution of frame-to-frame step lengths in the x and y directions. With 107 particles and 61 step intervals per particle in x and y, we obtained a list of 13 054 individual displacements which we plotted (see Fig. 6) as a histogram and normalized by dividing by the total number of particles. If we fit this distribution to Eq. (5), we obtain a self-diffusion constant of

$$D = (0.396 \pm 0.06)\ \mu\text{m}^2/\text{s} \quad \text{(uncorrected)}. \tag{19}$$

Following the analysis in Sec. IV A, we have to correct for hydrodynamic effects by increasing the diffusivity by 1.4% to yield a final value of D of

$$D = (0.402 \pm 0.06)\ \mu\text{m}^2/\text{s} \quad \text{(corrected)}. \tag{20}$$

Therefore, this method yields a value for Boltzmann's constant of

$$k = \frac{6\pi\eta a}{T} D = (1.22 \pm 0.18) \times 10^{-23}\ \text{J/K}, \tag{21}$$

where the uncertainty has been obtained by adding errors in quadrature.

Although this value of k is somewhat low, it is consistent with the accepted value of 1.38×10^{-23} J/K. To check whether this low value was due to a short time step, we looked at distributions for longer times (0.4 and 2.0 s) and found similar low values for k.

This low value of k suggests that an excellent variation of this experiment would be to plot the step probability distributions for many different time steps and compare the values of k obtained to the method outlined in Sec. IV A. Does the result we found continue to hold? It would also increase conceptual understanding to ask students to predict and sketch how they expect these probability distributions to change as the time interval increases.

V. CONCLUSIONS

The most difficult aspect of our experiment is creating an observation cell with no noticeable drift and with a sufficient and quantifiable depth to allow us to ignore sphere-wall interactions. We need to improve the method we used, because we did not visually notice the drift in slides one and four until we analyzed and compared them to a simulated data set.

Because the viscosity of water is a sensitive function of temperature, the value we obtained for k is very dependent on both the data in Table I and our method of interpolation. Although an exponential function appears to provide a good fit from 10 °C to 40 °C, it would be desirable to have viscosity data that was sampled at smaller temperature intervals than 10 °C.

Although the values for k are consistent with the accepted value, we remain puzzled by the low value obtained via the probability distribution. Nevertheless, we have obtained a value for k consistent with the accepted value. Our experiment serves to introduce statistical mechanics concepts in an engaging way into an upper level undergraduate setting while simultaneously determining a fundamental constant of nature.

We realize that although the hardware for this experiment is relatively inexpensive, the software (LabView and the imaging software add on) is not. Our particular combination of software was used because we already owned it and had previously developed tracking routines for an unrelated research project. If cost is an issue, a less expensive route may be to use IDL.[24] There are already routines available[25] to do particle tracking with IDL, so this method might prove worthwhile to those not already invested in LabView.

ACKNOWLEDGMENTS

We would like to acknowledge the extremely helpful discussions with Les Blatt at Clark University as well as Robert Coakley at the University of Southern Maine. Original support at Clark University for the creation of this laboratory came from NSF Grant No. DUE-925 4222, and further support came from the University of Southern Maine Faculty Senate.

[a]Electronic mail: pauln@maine.edu (URL: www.usm.maine.edu/~pauln/).

[1]Robert Brown, in *The World of the Atom*, edited by H. Boorse and L. Motz (Basic Books, New York, 1966), Vol. 1, pp. 206–212.
[2]Albert Einstein, "Über die von der molekularkinetischen Theorie der Wärme geforderte Bewegung von in ruhenden Flüssigkeiten suspendierten Teilchen," Ann. Phys. (Leipzig) **17**, 549–560 (1905).
[3]John Stachel, editor, *Einstein's Miraculous Year* (Princeton University Press, Princeton, NJ, 1988), pp. 85–98. This book includes a translation of Ref. 2.
[4]Albert Einstein, *Investigations on the Theory of the Brownian Movement* (Dover, New York, 1956).
[5]J. Perrin, *Atoms* (Ox Bow Press, New York, 1990), pp. 109–133.
[6]See ⟨http://www.nobel.se/physics/laureates/1926/index.html⟩ for Perrin's Nobel Prize acceptance speech.
[7]S. Inoué, *Video Microscopy* (Plenum, New York, 1986), pp. 111–115.
[8]J. Crocker and D. Grier, "Methods of digital video microscopy for colloidal studies," J. Colloid Interface Sci. **179**, 298–310 (1996).
[9]H. Graden Kirksey, "Brownian motion: A classroom demonstration and student experiment," J. Chem. Educ. **65**, 1091–1093 (1988).
[10]H. Kruglak, "Boltzmann's constant: A laboratory experiment," Am. J. Phys. **41**, 344 (1973).
[11]Reese Salmon, Candace Robbins, and Kyle Forinash, "Brownian motion using video capture," Eur. J. Phys. **23**, 249–253 (2002).
[12]See ⟨http://www.ni.com/⟩ for more information. We use LabView 6.0 and their IMAQ imaging software. The latter adds a host of imaging routines into the LabView environment. Each package costs $1296.75 (academic cost) for a single license. If used for teaching purposes only, National Instruments offers a departmental site license for $3995.
[13]R. P. Feynman, *The Feynman Lectures in Physics* (Addison-Wesley, Reading, MA, 1963), Vol. 1, pp. 41-8–41-10.
[14]F. Reif, *Fundamentals of Statistical and Thermal Physics* (McGraw-Hill, New York, 1965), pp. 565–567. Reif's classic text goes into a more in depth discussion of Brownian motion.
[15]Essentially any video card that allows for NTSC video input should suffice; these cards typically come with software to create videos. On newer machines, it is possible to use USB capable cameras, negating the need for a separate capture card.
[16]See ⟨http://www.bangslabs.com/⟩.
[17]E. Dufresne, D. Altman, and D. Grier, "Brownian dynamics of a sphere between parallel walls," Europhys. Lett. **53**, 264–270 (2001).
[18]J. Crocker, "Measurement of the hydrodynamic corrections to the Brownian motion of two colloidal spheres," J. Chem. Phys. **106**, 2837–2840 (1997).
[19]Available from Physics Academic Software, ⟨http://webassign.net/pasnew/⟩.
[20]ImageJ is available for free at ⟨http://rsb.info.nih.gov/ij/⟩.
[21]The Labview routines as well as sample data are available at ⟨http://www.usm.maine.edu/~pauln/⟩; follow the Brownian motion link.
[22]Igor Pro is a fast, powerful, programmable scientific graphics package (with a C-like syntax) available from ⟨http://www.wavemetrics.com/⟩.
[23]*CRC Handbook of Chemistry and Physics*, 72nd ed., edited by David R. Lide (CRC, Boca Raton, FL, 1991).
[24]IDL is available from Research Systems at ⟨http://www.rsinc.com/⟩.
[25]See ⟨http://glinda.lrsm.upenn.edu/~weeks/idl/⟩ for a set of IDL routines to do particle tracking.

THE SOCIAL SYSTEM OF SCIENCE

The social system of science begins with the apprenticeship of the graduate student with a group of his peers and elders in the laboratory of a senior scientist; it continues to collaboration at the bench or the blackboard, and on to formal publication—which is a formal invitation to criticism. The most fundamental function of the social system of science is to enlarge the interplay between imagination and judgment from a private into a public activity. The oceanic feeling of well-being, the true touchstone of the artist, is for the scientist, even the most fortunate and gifted, only the midpoint of the process of doing science.

Horace Freeland Judson, *The Search for Solutions* (Playback Associates, 1980). Reprinted in *The World Treasury of Physics, Astronomy, and Mathematics* (Little, Brown and Company, Boston, MA, 1991), p. 786.